ELSEVIER

Journal of Nuclear Materials 288 (2001) 202–207

journal of nuclear materials

www.elsevier.nl/locate/jnucmat

The effects of tungsten addition on the microstructural stability of 9Cr–Mo Steels

S.G. Hong, W.B. Lee, C.G. Park *

Center for Advanced Aerospace Materials, Pohang University of Science and Technology (POSTECH), San 31 Hyoja-Dong, Nam-Gu, Pohang, Kyungbuk 790-784, South Korea

Received 17 February 2000; accepted 13 October 2000

Abstract

The effects of tungsten addition on the microstructure and high-temperature tensile strength of 9Cr–Mo steels have been investigated by using three different steels: M10 (9Cr–1Mo), W18 (9Cr–0.5Mo–1.8W), and W27 (9Cr–0.1Mo–2.7W) steels. The tungsten-added 9Cr steels have revealed better high-temperature tensile strength. Microchemical analysis for $(Cr,Fe)_2$ (C,N) revealed that the tungsten addition increased the Cr/Fe ratio, which resulted in the lattice expansion of $(Cr,Fe)_2$ (C,N), and then the enhanced pinning effect on the glide of dislocation. In addition, in M10 steel, the $M_{23}C_6$ carbides quickly grew and agglomerated, while the tungsten-added 9Cr steels revealed a fine and uniform distribution of $M_{23}C_6$ carbides. Dislocation recovery during tempering treatments was delayed in tungsten-added 9Cr steels, which was correlated with the stabilized precipitates and the decreased self-diffusivity of iron. It is, thus, believed that the excellent high-temperature tensile strength of tungsten-added 9Cr steels is attributed to the stabilized M_2X carbo-nitrides and $M_{23}C_6$ carbides and the decreased self-diffusivity of iron.

PACS: 61.16.Bg; 62.20.-x

1. Introduction

Ferritic/martensitic steels have been considered as useful candidate materials for fossil-fueled power plants and fusion reactors, because of their high thermal conductivity and low thermal expansion coefficient in comparison to austenitic steels. These properties are favorable for application to various high-temperature plants. These days, in order to improve the thermal efficiency of a steam turbine in power plants, ultra-supercritical boilers require enhanced steam conditions of increased pressure and temperature. To meet these demands, several advanced types of 9%Cr steels are now being developed with the addition of more than 1.5% tungsten [1–5]. Although the tungsten addition is known to improve the high-temperature strength of 9Cr steel, the detailed mechanism for the improved mechanical properties is not well understood.

The objective of present study is, thus, to identify and to correlate between the effects of tungsten addition on the microstructural stability and the mechanical properties in 9Cr–Mo steels. In the present paper, the effect of tungsten addition on microstructural stability was examined with a variation of tempering conditions. Special attention was given to progressive changes in dislocation structure as well as to the nature and distribution of precipitates and their influences on the stability of the lath morphology.

2. Experimental procedure

The chemical composition of the steels examined in this study is shown in Table 1. The W was added by 0–2.7 wt% to the 9Cr steels, with a decrease in Mo content from 1.02 to 0.115 wt%, which were denoted as M10, W18 and

* Corresponding author. Tel.: +82-562 2792 139; fax: +82-562 2792 399.

E-mail address: cgpark@postech.ac.kr (C.G. Park).

0022-3115/01/$ - see front matter
PII: S0022-3115(00)00558-4

Table 1
Chemical composition of the steels examined in the present study (wt%)

Specimen	Composition									
	C	Si	Mn	Cr	Mo	W	V	Nb	B	N
M 10 (9Cr–1Mo)	0.110	0.070	0.45	8.85	1.02	–	0.20	0.069	0.007	0.047
W 18 (9Cr–0.5Mo–1.8W)	0.103	0.088	0.45	8.61	0.50	1.75	0.22	0.065	0.0062	0.050
W27 (9Cr–0.1Mo–2.7W)	0.110	0.088	0.44	8.88	0.115	2.7	0.21	0.069	0.0044	0.045

W27, respectively. The specimens were prepared by vacuum induction melting to ingnots, homogenized at 1250°C for 2 h, hot rolled to about 13 mm in thickness, and then normalized at 1050°C for 1 h. Then tempering was performed for 1 hour at various temperatures ranging from 600°C to 800°C followed by air-cooling.

Tensile tests were performed at a temperature of 600°C and a nominal strain rate of 5×10^{-4}/s on the specimens with a gage section of $20 \times 5 \times 3$ mm; the gage length was parallel to the rolling direction.

Microstructural examination and microchemical analysis were performed on the heat-treated specimens in the form of thin foils and extraction replicas using a philips CM30 (300 kV) TEM equipped with an energy-dispersive spectrometer (EDS). TEM thin foil specimens were prepared in a twin jet polisher operated at a moderate jet speed with an electrolyte of picric acid–HCl–ethanol at −20°C. The extraction replicas for precipitates in the steels were prepared by mechanical polishing and modified marble's etching method followed by carbon coating.

3. Results

3.1. Mechanical properties

A high-temperature (600°C) mechanical properties of M10, W18 and W27 steels are plotted in Fig. 1 as a function of tempering temperature. Mechanical properties of these steels were found to be affected by the amount of tungsten added to 9Cr–Mo steels. That is, the high-temperature tensile strength increased, but the elongation decreased, with increasing tungsten content at all tempering temperature ranges examined. The elongation of the W27 steel was less than that of the M10 steel, but similar to that of W18 steel. This result indicated that the W27 steel exhibited higher tensile strength and reasonably acceptable ductility in comparison to the others.

3.2. Microstructure

The 9% Cr steels are generally used in normalized and tempered condition. M10 and W18 steels exhibited only martensite in normalized condition, while W27 steel showed dual phase structure with martensite and δ-ferrite as shown in Fig. 2(a)–(c). The average lath width of martensite was about 0.4 μm (Fig. 2(a)–(c)) and the average grain size of prior austenite was about 20 μm, which were fairly similar in all the steels.

In commercial practice, normalized steels are usually tempered at temperatures between 650°C and 800°C in order to increase their toughness and precipitation hardening. Very little or no obvious difference in dislocation structure was observed in the M10 steel tempered at 600°C and 650°C. In comparison, 700°C tempering resulted in a reduced dislocation density and the initiation of lath break-up as shown in Fig. 3(a). As

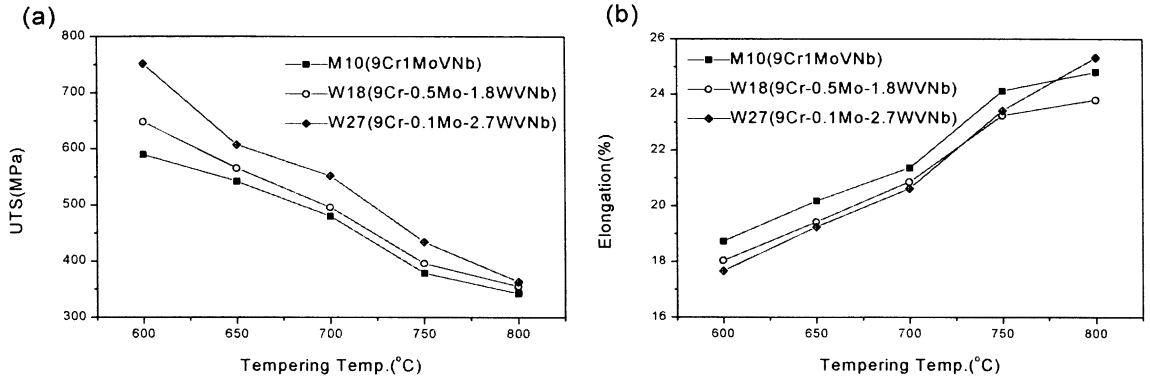

Fig. 1. High-temperature tensile properties of M10, W18 and W27 steels: (a) ultimate tensile stress; (b) elongation.

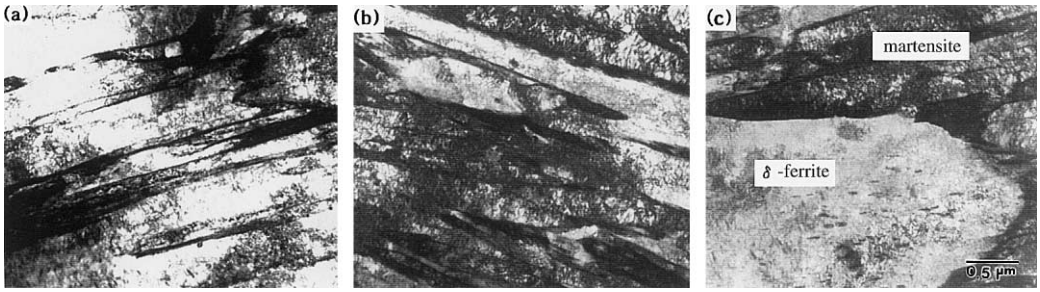

Fig. 2. TEM micrographs showing the typical microstructure of (a) M10, (b) W18 and (c) W27 steels only normalized at 1050°C.

the tempering temperature of M10 steel was increased to 750°C and 800°C, the lath morphology was transformed to dislocation arrays lying transverse to longitudinal axes of the laths (indicated by arrows in Fig. 3(b)), followed by the formation of an equiaxed grain structure with a low dislocation density (Fig. 3(c)). However, in the W18 steel, which consisted of lath subgrains with a high density of dislocation or dislocation network even after 700°C tempering, a significant recovery of excess dislocations started to occur on 750°C tempering, as shown in Fig. 3(e). Even under 800°C tempering treatment, the lath morphology observed in W18 steel was stable and remained elongated (Fig. 3(f)). It was, thus, summarized that the break-up of lath martensite started under the 700°C tempering in M10 steel, but under the 750°C tempering in W18 steel, which suggested a retardation of dislocation recovery due to the tungsten addition.

3.3. Precipitation

The identification of precipitates was carried out by microdiffraction and EDS analysis on extraction replicas. Upon being normalized at 1050°C, all the steels examined exhibited lath martensite containing fine $(Fe,Cr)_3C$ particles. In addition, equiaxed particles identified as Nb(C,N), ranging from 0.1 to 0.2 μm in diameter, were observed in normalized condition of M10, W18 and W27 steels (Table 2). The size of Nb(C,N) suggests that they are residual precipitates undissolved during the austenitization treatment. Subsequent tempering caused the precipitation of additional carbo-nitrides and carbides, such as $(Cr,Fe)_2(C,N)$, $M_{23}C_6$ (M = Cr, Fe, Mo) and MX (M = V, Nb; X = C, N) with the dissolution of $(Fe,Cr)_3C$, as observed in previous tests by others [2,6,7].

Precipitation sequence primarily depends on the chemical composition of the steel. Furthermore, the relative diffusivities of the alloy elements and the ease of nucleation are also important factors to be considered in determining which carbide phases are favored. The formation of $(Cr,Fe)_2(C,N)$ as the first alloy carbide during tempering treatment seemed quite reasonable because of the easy availability and higher diffusivity of Cr compared to other metallic elements as reported by

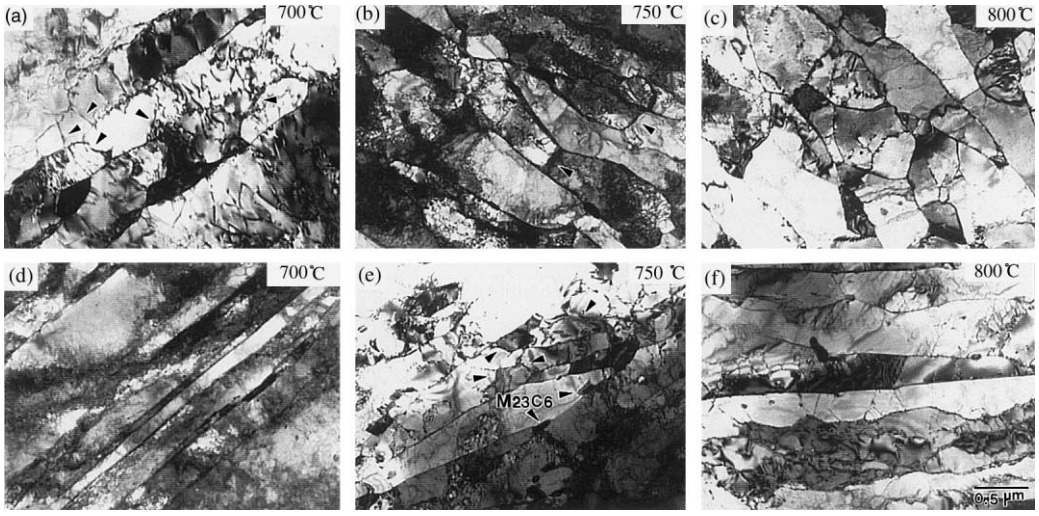

Fig. 3. TEM micrographs showing typical microstructure of ((a)–(c)) M10 and ((d)–(f)) W18 steels tempered at ((a), (d)) 700°C, ((b), (e)) 750°C and ((c), (f)) 800°C.

Table 2
Carbides and carbo-nitrides identified under various tempering conditions

Condition	Specimen		
	M10	W18	W27
Normalized	Nb(C,N), $(Fe,Cr)_3C$	Nb(C,N), $(Fe,Cr)_3C$	Nb(C,N), $(Fe,Cr)_3C$
600°C tempered	Nb(C,N), $(Cr,Fe)_2(C,N)$	Nb(C,N), $(Cr,Fe)_2(C,N)$	Nb(C,N), $(Cr,Fe)_2(C,N)$
650°C tempered	Nb(C,N), $(Cr,Fe)_2(C,N)$, $M_{23}C_6$	Nb(C,N), $(Cr,Fe)_2(C,N)$	Nb(C,N), $(Cr,Fe)_2(C,N)$
700°C tempered	Nb(C,N), $M_{23}C_6$, MX	Nb(C,N), $(Cr,Fe)_2(C,N)$, $M_{23}C_6$, MX	Nb(C,N), $(Cr,Fe)_2(C,N)$, $M_{23}C_6$, MX
750°C tempered	Nb(C,N), $M_{23}C_6$, MX	Nb(C,N), $M_{23}C_6$, MX	Nb(C,N), $M_{23}C_6$, MX
800°C tempered	Nb(C,N), $M_{23}C_6$, MX	Nb(C,N), $M_{23}C_6$, MX	Nb(C,N), $M_{23}C_6$, MX

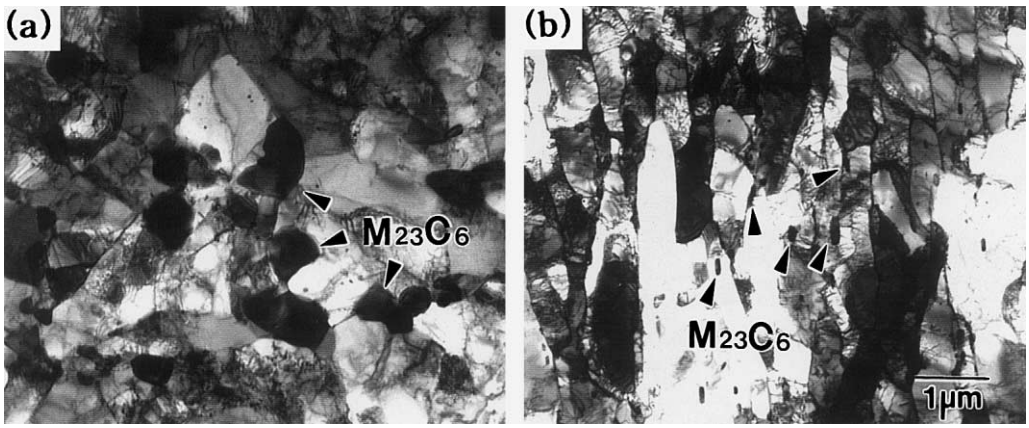

Fig. 4. TEM micrographs showing typical microstructure of (a) M10 and (b) W18 steels tempered at 800°C.

Pickering [8]. This $(Cr,Fe)_2(C,N)$ started to disappear under the 650°C tempering in M10 steel, but was stable up to the 700°C tempering in W18 and W27 steels (Table 2). The tempering at higher temperature produced equiaxed carbides nucleated at lath interfaces (Fig. 4), which were confirmed as Cr-rich $M_{23}C_6$.

4. Discussion

The effects of tungsten addition on the microstructural stability of 9Cr–Mo steels were considered from the correlation between precipitation of carbides or carbo-nitrides and dislocation recovery.

It is generally recognized that one or more transitional carbides may form during the tempering of alloy steels. Precipitates in 9Cr steels where chromium is the strongest carbide-forming element, have been reported as $(Fe,Cr)_3C$, M_7C_3 and $M_{23}C_6$ [9,10]. $(Fe,Cr)_3C$ observed in normalized 9Cr steels is known to precipitate during air-cooling after austenizing as a result of auto-tempering. Although it was known that the subsequent tempering of 9Cr steels precipitated M_7C_3 and $M_{23}C_6$ carbides, the M_7C_3 carbides were not observed in the present alloy steels. Instead, M_2X carbo-nitrides were formed in these present alloy steels. It would appear that the presence of nitrogen, often occurring in 9Cr steels, forms a hexagonal M_2X carbo-nitrides preferably rather than the rhombohedral M_7C_3 carbides, which may be regarded as a defect lattice having interstitial vacancies. The nitrogen fills the interstitial vacant sites and changes the crystallography from rhombohedral structure (M_7C_3) to hexagonal structure (M_2X) [11].

Quantitative EDS analysis of M_2X type carbo-nitride, $(Cr,Fe)_2(C,N)$ revealed that the Cr/Fe ratio of the M_2X carbo-nitride was higher in the W18 steel than in the M10 steel, as shown in Fig. 5. The Cr/Fe ratio for the W18 steel tempered at 600°C and 650°C was about 7.8 and 3.7 and about 3.2 and 2.2 for the M10 steel, respectively. These results indicate the relatively lower solubility of iron in M_2X formed in the tungsten-added steels and are quite consistent with the retardation of iron diffusion due to tungsten addition, as reported by Cermak et al. 12. This relative chromium enrichment due to iron deficiency can cause the increase in lattice parameter of M_2X phase (radius of Cr, 1.85 Å; radius of Fe, 1.72 Å). The tempering resistance of 9Cr steels can be generally improved by increasing coherent strains or

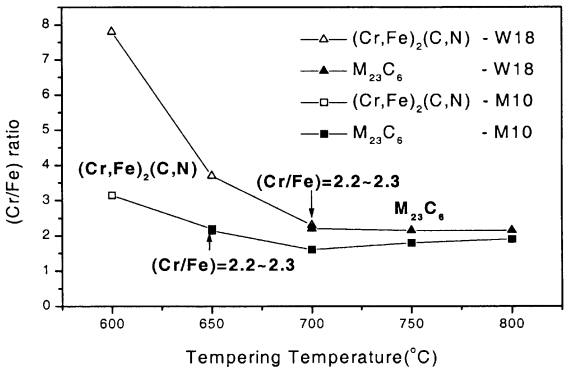

Fig. 5. Cr/Fe ratio of $(Cr,Fe)_2(C,N)$ and $M_{23}C_6$.

volume fraction of precipitates. Particularly, the increase of coherent strains is obtainable by increasing the lattice parameter of precipitates. This increase in lattice parameter can enhance the stability and the strengthening effect of M_2X carbo-nitrides and then effectively restricts dislocation recovery. In addition, the recovery of excess dislocations occurs mainly by self-diffusion of iron, and it was reported that tungsten markedly decreased the self-diffusivity of iron in Fe–W binary alloys 12. It is, thus, considered that the delayed initiation of lath break-up in tungsten-added steels as observed in Fig. 3, is caused by the enhanced strengthening effect of M_2X carbides and the decrease of self-diffusivity of iron.

When the steels were tempered at higher temperatures, $M_{23}C_6$ carbides were generally observed rather than M_2X carbo-nitrides. That is, the M_2X carbo-nitrides have started to disappear and been replaced by the $M_{23}C_6$ carbides at 650°C tempering in M10 steel and at 700°C tempering in W18 and W27 steels. The compositional changes of M_2X carbo-nitrides and $M_{23}C_6$ carbides were plotted in Fig. 5. As shown in Fig. 5 and Table 2, it was considered that the replacement of M_2X by $M_{23}C_6$ was correlated with the compositional change of precipitates, Cr/Fe ratio. That is, in M10 steel tempered at 600°C, the Cr/Fe ratio of M_2X carbo-nitrides was about 3.2, but as tempering temperature increased to 650°C, this ratio decreased to 2.2–2.3, at which $M_{23}C_6$ carbides simultaneously started to form at lath and grain boundaries. It is, thus, considered that when the Cr/Fe ratio of M_2X carbo-nitrides finally got to about 2.2, the M_2X carbo-nitrides were no more stable and then replaced by $M_{23}C_6$ carbides.

The replacement of M_2X carbo-nitrides by $M_{23}C_6$ carbides occurred at higher tempering temperature in the W18 steel than in M10 steel, that is, at 650°C in the M10 steel and at 700°C in the tungsten-added steels. $M_{23}C_6$ carbides of M10 steel replaced at lower tempering temperature were quickly coarsened and agglomerated during the tempering at a higher temperature of 800°C (Figs. 4(a) and 6(a)), while those of tungsten-added steels replaced at higher tempering temperature exhibited a fine and uniform distribution even after 800°C tempering (Figs. 4(b) and 6(b)). Furthermore, as shown in Fig. 7, it was considered that the increased partition of heavy element, W + Mo into $M_{23}C_6$ carbides of tungsten-added steels could make $M_{23}C_6$ carbides more stable [10]. Since the carbides are primarily responsible for the pinning of lath boundaries, the coarsening and spheroidization of $M_{23}C_6$ carbides can easily increase the mobility of lath interface to result in the break-up of lath structure. In fact, in the M10 steel tempered at 800°C exhibiting significantly coarsened $M_{23}C_6$ carbides, the lath structure was considered to grow into an equiaxed subgrain structure during tempering, as shown in Fig. 3(c). However, in the tungsten-added 9Cr steels exhibiting the uniform distribution of find $M_{23}C_6$ carbides, a stabilized lath morphology was found, as shown in Fig. 3(f).

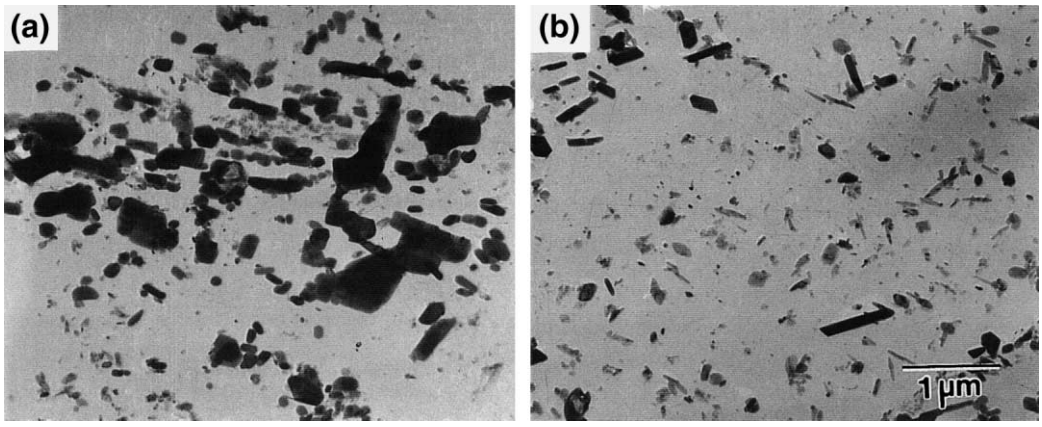

Fig. 6. TEM micrographs of extraction replica showing $M_{23}C_6$ carbides distribution observed in (a) M10 and (b) W18 steels tempered at 800°C.

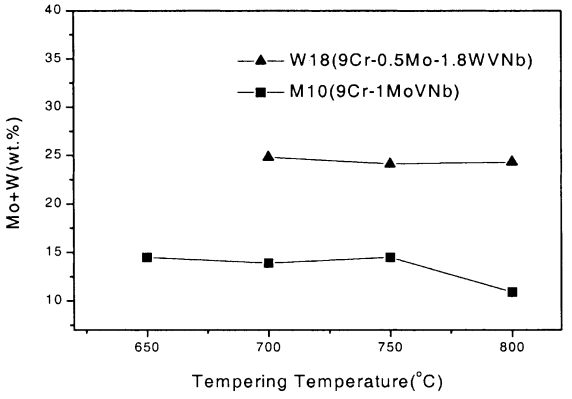

Fig. 7. The amount of Mo + W within $M_{23}C_6$ in M10 and W18 steels.

It is, thus, postulated that the stabilized microstructure of tungsten-added 9Cr steels is attributed to the stabilization of M_2X carbo-nitrides, the uniform distribution of fine $M_{23}C_6$ carbides and the retardation of dislocation recovery. Therefore, it is considered that this stabilized microstructure could be the reason for the enhanced high-temperature tensile strength of the tungsten-added 9Cr steels.

5. Conclusions

1. M_2X carbo-nitride revealed a higher Cr/Fe ratio in tungsten-added 9Cr steels than that in 9Cr–Mo steel resulting in an enhanced strengthening of M_2X through the lattice expansion.
2. In M10 steel, the $M_{23}C_6$ carbides quickly grew and agglomerated, while in the tungsten-added 9Cr steels, the coarsening of $M_{23}C_6$ carbides was restricted resulting in a fine and uniform distribution of $M_{23}C_6$ carbides.
3. Dislocation recovery and polygonization of lath morphology were proceeded by increasing tempering temperature. However, the tungsten addition to 9Cr steels delayed these processes resulting in the stabilized microstructure of tungsten-added 9Cr steels.
4. The stabilized microstructure of tungsten-added 9Cr steels is attributed to the stabilization of M_2X carbo-nitrides, the uniform distribution of fine $M_{23}C_6$ carbides and the retardation of dislocation recovery. It is, thus, considered that this stabilized microstructure could be the reason for the enhanced high-temperature tensile strength of the tungsten-added 9Cr steels.

Acknowledgements

The authors thank Korea Science and Engineering Foundation (KOSEF) for the financial support (96-0300-01-01-3).

References

[1] T. Fujida, ISIJ Int. 32 (1992) 175.
[2] F. Abe, S. Nakazawa, Metall. Trans. A. 23A (1992) 3025.
[3] H. Yasuda, M. Sakakibara, T. Takahashi, H. Naoi, H. Masumoto, Therm. Nucl. Power 39 (1988) 517.
[4] M. Sakakibara, H. Masumoto, T. Ogawa, T. Takahashi, T. Fujita, Therm. Nucl. Power 38 (1987) 841.
[5] J.S. Park, K.A. Lee, C.S. Lee, Metall. Mater. 5 (6) (1999) 559.
[6] B.J. Wendell, C.R. Hills, D.H. Polonis, Metall. Trans. A. 22A (1991) 1049.
[7] S. Saroja, P. Parameswaran, M. Vijayalakshmi, V.S. Raghunathan, Acta Metall. Mater. 43 (1995) 2985.
[8] F.B. Pickering, Physical Metallury and the Design of Steels, Applied Science, London, 1978, p. 136.
[9] J. Nutting, in: J.W. Davis, D.J. Michel (Eds.), Proceedings of the Topical Conference on Ferritic Alloys for Use in Nuclear Energy Technologies, TMS-AIME, Warrendale, PA, 1984, p. 3.
[10] F. Abe, H. Araki, T. Noda, Metall. Trans. A. 22A (1991) 2225.
[11] A. Strang, D.J. Gooch, Microstructural Development and Stability in High Chromium Ferritic Power Plant Steels, Institute of Materials, London, 1997, p. 11.
[12] J. Cermak, J. Kucera, B. Million, J. Krumpos, Kov. Mater. 18 (1980) 537.